ATMOSPHERIC ENVIRONMENT: X 6 (2020) 100072

Contents lists available at ScienceDirect

Atmospheric Environment: X

journal homepage: http://www.journals.elsevier.com/atmospheric-environment-x

Mapping the deposition of ^{137}Cs and ^{131}I in North America following the 2011 Fukushima Daiichi Reactor accident

I. Hoffman [a,*], A. Malo [b], P. Mekarski [a], J. Yi [a], W. Zhang [a], N. Ek [b], P. Bourgouin [c], G. Wotawa [d], K. Ungar [a]

[a] Radiation Protection Bureau, Health Canada, 775 Brookfield Rd, Ottawa, ON, Canada
[b] Canadian Meteorological Centre, Environment and Climate Change Canada, 2121 Trans-Canada Highway, North Service Road, Dorval, QC, Canada
[c] Comprehensive Nuclear-Test-Ban Treaty Organization Preparatory Commission, PO Box 1200, 1400, Vienna, Austria
[d] Zentralanstalt für Meteorologie und Geodynamik, Hohe Warte 38, 1190, Vienna, Austria

ARTICLE INFO

Keywords:
Fukushima reactor accident
Deposition
Environmental radioactivity
Aerosol
Atmospheric transport and dispersion modelling

ABSTRACT

The 2011 Fukushima Daiichi Reactor accident generated a large data set of global radionuclide observations. Frequent observations of xenon, caesium and iodine radioisotopes provided an opportunity to examine the performance of inter-continental scale meteorological models, in particular, the important mechanisms of in-cloud scavenging, precipitation, and deposition. Previous studies investigated these phenomena over short range, but this is the first time a global, coordinated surveillance system and in particular, a non-scavenged noble gas data set was available for use in such a study. Since particle size distributions are very different at long range, the parametrization of the deposition is important for accurate atmospheric modelling. The accuracy of these models are crucial in the Comprehensive Nuclear-Test-Ban Treaty (CTBT) context where discrimination of local and distant civilian sources from a potential nuclear test is a challenging problem. Beyond the CTBT context, accurate prediction of deposition is important for emergency and consequence management of nuclear emergencies, allowing a small set of data, combined with an appropriate model to represent a much larger domain, even up to continental scales. The modelling results for ground deposition and airborne activity of radiocaesium and radioiodine are presented and validated against the actual measurements.

1. Introduction

The 2011 Fukushima Daiichi reactor accident released large quantities of radioactive debris into the environment which initiated concerns globally about the long range atmospheric transport of contaminants and associated risks. In Canada, the immediate concern in the accident aftermath was for the quantity and species of aerosol radionuclides released as they would be the first to affect Canadians in the accident vicinity and would also be the first to arrive on the North American continent. Early simulations showed a 5 d to 6 d atmospheric transport time from the damaged reactors to Canadian shores. Considering potential exposure and the associated health risks, the two dominant species, ^{137}Cs and ^{131}I, were the initial focus of assessments. Once these isotopes were released, they travelled great distances through the atmosphere and were removed through the processes of decay and wet and dry deposition. From a health risk perspective, the process of wet deposition is extremely important as radioactive debris will accumulate in areas of precipitation, which were not necessarily the areas closest in proximity to the accident site or even in those areas where the airborne aerosol concentrations were greatest. Additionally, once the behaviour of these two isotopes were understood, their results could be scaled, if necessary, to other isotopes of radioprotective importance such as: ^{134}Cs, ^{132}I, and ^{133}I.

Reconstructing the environmental pathways of these isotopes are important factors to consider in emergency response and consequence management phases. During the emergency response phase, it can inform and validate the emergency response actions, while in the consequence management phase, it enables health impact assessments that consider the relevant exposure pathways and can help guide any necessary decontamination efforts. Previous studies have modelled the Fukushima deposition process in detail over Europe and Asia (Evangeliou et al., 2015), while others have focused in great detail on deposition in Japan (Korsakissok et al., 2013; Morino et al., 2011; Katata et al., 2015; Draxler et al., 2015). Past accidents such as Chernobyl have

* Corresponding author.
E-mail address: ian.hoffman@canada.ca (I. Hoffman).

https://doi.org/10.1016/j.aeaoa.2020.100072
Received 24 October 2019; Received in revised form 19 March 2020; Accepted 25 March 2020
Available online 18 April 2020

also been studied – in particular the deposition and atmospheric residence times (Uematsu et al., 1988). This paper studies the deposition and atmospheric residence of ^{137}Cs and ^{131}I over North America addressing this missing region in the Northern Hemisphere. This is the first study to use radioxenon measurements as a normalizing factor in the deposition analysis to improve deposition modelling.

The deposition of ^{137}Cs is relatively straightforward to model at least in comparison to ^{131}I. In Atmospheric Transport and Dispersion Modelling (ATDM), ^{137}Cs can be modelled purely as a particulate aerosol, while ^{131}I is extremely complex environmentally, as there are two different phases of the material (gaseous and particulate) with a conversion process between gaseous and particulate forms happening continuously in the environment. The approach employed to model this challenging behaviour is discussed in Section 2.4.

2. Method

2.1. Source term and receptors

To accurately model and parametrize the wet and dry deposition of ^{137}Cs and ^{131}I using Fukushima debris, a source term was required. The source term used for this study was derived by the Japanese Atomic Energy Agency (JAEA) (Chino et al., 2011), which was later modified by further studies (Terada et al., 2012). A temporal plot of the source term model is shown in Fig. 1 for both ^{137}Cs and ^{131}I. It was used as the atmospheric injection source term by the Modele Lagrangian de Dispersion de Particules (MLDP) ATDM of the Canadian Meteorological Centre (CMC). The goal was to determine the residence time of the gaseous and particulate iodine in the atmosphere and to predict the ground deposition of ^{137}Cs and ^{131}I in Canada for future health impact studies. The CTBT monitoring sites used to evaluate the ATDM and subsequently used to predict the deposition are shown in Fig. 2.

2.2. Transport and dispersion modelling

The dispersion modelling was performed at CMC using the long-range MLDP Lagrangian model that is a Canadian dispersion code. Dispersion is estimated by calculating the trajectories of a very large number of air particles (also called parcels or fluid elements), simulating the processes of advection and diffusion. Large scale transport is handled

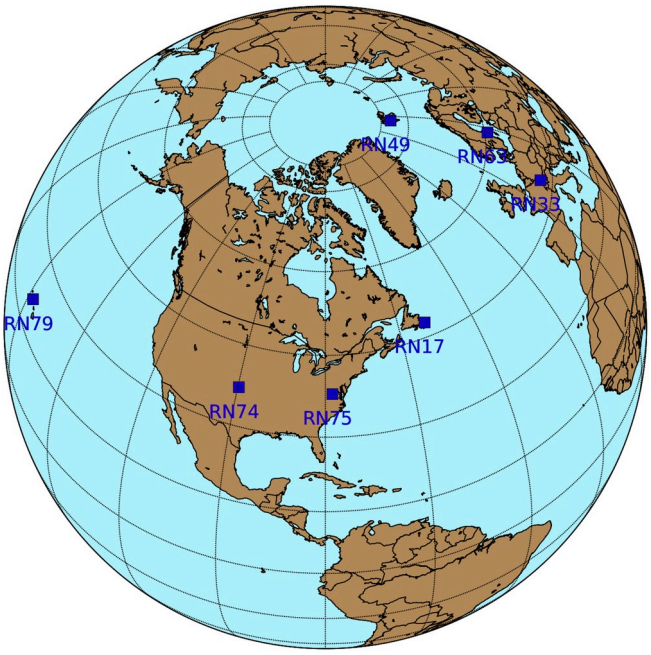

Fig. 2. The CTBTO IMS locations used in the deposition evaluation: RN17 St. John's, Canada; RN33 Schauinsland, Germany; RN49 Spitsbergen, Norway; RN63 Stockholm, Sweden, RN74 Ashland, USA; RN75 Charlottesville, USA; RN79 Oahu, USA. The sites chosen all had noble gas measurement capability, so that a decay/aerosol removal model could be constructed.

by calculating the displacement due to the synoptic component of the wind field and diffusion through discretized stochastic differential equations to account for the unresolved turbulent motions. MLDP is an off-line model that uses the full 3-D meteorological fields provided by the Canadian Global Environmental Multiscale Model (GEM) numerical weather prediction system. Therefore, fields of wind, moisture, temperature and geopotential heights must be provided to the dispersion model. These fields are normally obtained from the Canadian GEM forecasts and objective analyses in either a global, regional or high resolution configuration. MLDP also accounts for physical removal effects such as radioactive decay, wet scavenging, dry deposition and

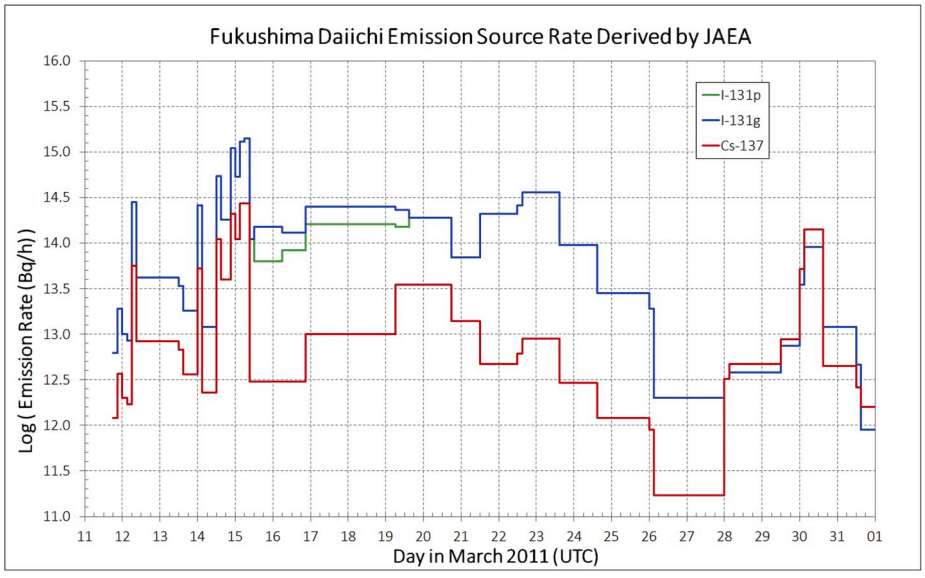

Fig. 1. The atmospheric source term inject used to project the reactor debris into the environment. This source term was used as the input into the MLDP model. Except for a small period between the 15 and 20 March, the particulate iodine source term was identical to the gaseous iodine source term.

gravitational settling by calculating the amount of material removed from the carrier particle when it travels in regions of the atmosphere where such processes are active. The domain over which the model was run is shown in Fig. 3. Further information on the MLDP model can be found in (D'Amours et al., 2015).

2.3. Collection and deposition

In this study, MLDP was run in forward (time) mode driven by analyzed meteorological fields available from GEM at 33 km (≈0.3°) horizontal grid mesh and at 6 h time intervals. In order to capture most of the cumulative effects of radioactive aerosol dispersion over North America, the model was integrated over a very long period, nine weeks, starting from the accident release time on March 11, 2011 at 18:00 UTC to May 16, 2011 at 00:00 UTC. This long duration simulation was sufficient to capture several circumglobal trips of the radioactive debris plume. The meteorological fields were pre-processed and interpolated over a northern hemispheric grid (polar stereographic projection) at a coarser spatial resolution, 100 km (≈1.0°) grid mesh. The model concentration and deposition output fields were also calculated on the same grid in order to minimize numerical noise at long range associated with a Lagrangian modelling approach and to obtain the average smoothed impact over Canada and the USA. A total of 30 non-uniform vertical levels were selected for the ATDM calculation including 14 levels within 2 km Above Ground Level (AGL) or below ≈800 hPa in order to properly resolve physical processes in the atmospheric boundary layer. The output near-surface concentrations (layer between surface and 200 m AGL) were averaged over a 12 h time period. The internal model time step was fixed at 10 min, and five million Lagrangian parcels were used for the simulation. Near-surface concentrations and total ground deposition were calculated using two different methods for the three radionuclides of interest: ^{137}Cs, particulate ^{131}I (I-131p), gaseous ^{131}I (I-131g), and ^{133}Xe.

2.3.1. Field measurements deposition

For the field measurement locations, the source term model was propagated using the MLDP model to the network of measurement sites operated on behalf of the CTBTO as shown in Fig. 2. From these predictions and actual measurements it was possible to derive local deposition coefficients.

When the Fukushima plume debris arrived at an IMS site, it was collected either using a particulate filtration system or a noble gas analyser. For the particulate debris, the collection system consists of an air sampler with particulate filter that operates on a daily duty cycle which typically samples in excess of 20000 m^3d^{-1}. After sampling, the filter rests on-site for 24 h to allow the short-lived radon progeny to decay before measurement with an on-site high-resolution gamma spectrometer. This rest period was designed to allow for enhanced sensitivity to nuclear-test debris. For this study, we assumed that all debris had the same origin time, which although not strictly accurate, is a reasonable approximation considering the half-lives, 30.08 a and 8.03 d, of ^{137}Cs and ^{131}I respectively and the long distance transport of the plume prior to sampling. As the Fukushima debris was released over a very short period, all reported activity concentrations used the beginning of the source term model as a reference time.

Furthermore, all the selected IMS locations had the capability to measure radioxenon gas concentrations. Although four different radioxenon species are quantifiable with the radioxenon analysers used in the IMS, this study only made use of ^{133}Xe. With the greatest sensitivity, ^{133}Xe is the most reliably measured species, and was used to normalize activity concentrations so that the deposition coefficient could be more reliably determined.

2.3.2. Model deposition

For the purely simulated deposition process, the MLDP model was used. In this model, wet deposition effects are computed using an in-cloud scavenging model scheme using the local cloud fraction, which is parametrized as a function of Relative Humidity (RH). Upon reaching the RH threshold barrier of 75%, the wet deposition process is activated. For dry deposition, which occurs when a simulated particle experiences a reflection at the ground surface, the process is parametrized by an absorption probability and a dry deposition velocity. The combination of these two processes are the main mechanisms of particle removal from the atmosphere, with wet scavenging being the dominant

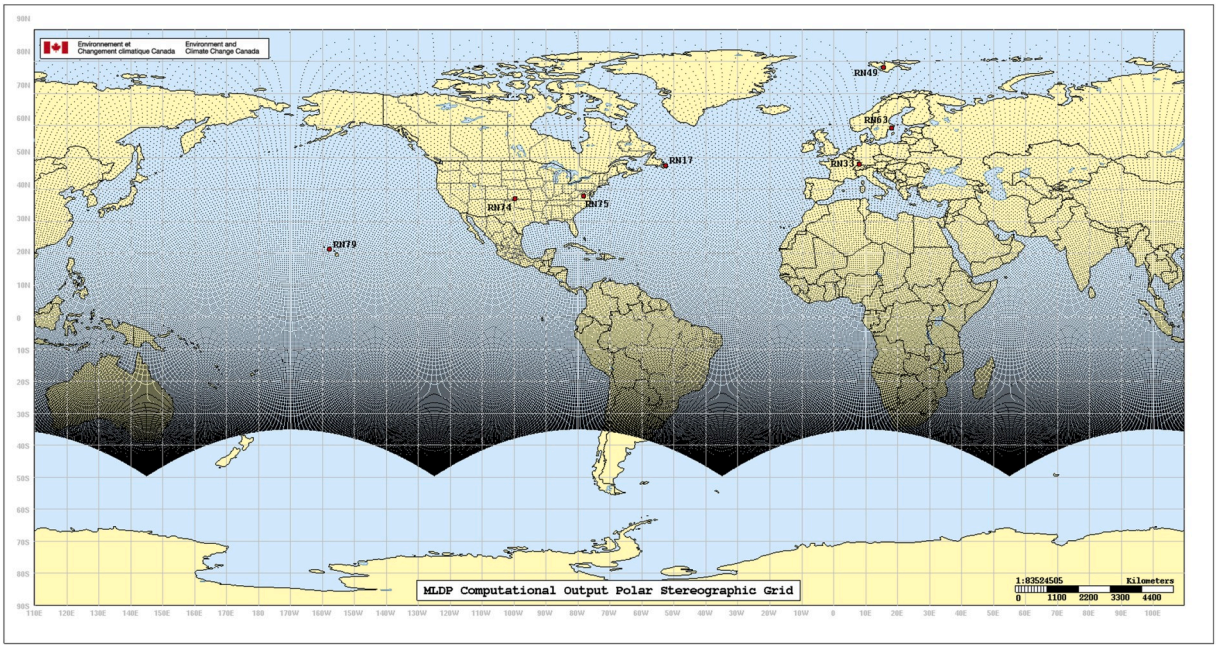

Fig. 3. The computational model grid domain (black dots) for the MLDP transport and deposition simulations is a polar stereographic grid at 100 km mesh at 60° N. The red dots are the CTBTO IMS measurement sites used in this study. The simulation was run for 65.25 d with 12 h output at 100 km resolution. (For interpretation of the references to colour in this figure legend, the reader is referred to the Web version of this article.)

mechanism by about an order of magnitude. Gravitational settling was not accounted for in the model runs. For the deposition modelling performed in this study, there was no decay applied to deposited particles. For ^{137}Cs, with a long half-life compared to the period of the study, this effect can be neglected, but for the ^{131}I results, the predicted deposition will be over-estimated.

The results of the simulated deposition were compared with those determined from field measurements for validation. The MLDP model could then be used to construct a deposition map over the entire North American continent.

2.4. Constructing a continental deposition map

To develop a deposition map of North America, a simple kinetic model was created to simulate the various atmospheric processes acting on the Fukushima debris. This model was similar to previous models used during the Chernobyl accident to model the deposition of ^{137}Cs and ^{131}I in the North Pacific (Uematsu et al., 1988), but incorporated the use of a noble gas normalizing factor. Fig. 4 shows a schematic of the model, illustrating the physical interactions of the aerosols and gases. In this model, all particulate monitoring data was decay-corrected to the reference time in a simplification of the actual release profile from the damaged reactors.

The behaviour of radioiodine in nuclear reactors and the environment is quite complex as various chemical and physical forms are involved depending on many variables such as formation temperature, reactor safety systems, and atmospheric chemistry. In a severe reactor accident, the radioiodine released exists as molecular iodine (vapour), organic iodide species (vapour) such as methyl iodide or as iodide salts (particulate) (Lebel et al., 2016). The variety of iodine species combined with the physical and chemical factors results in a situation of imperfect information that makes the atmospheric transport and deposition modelling of ^{131}I challenging.

One of the key unknowns in the model was the relative amounts of particulate and gaseous ^{131}I. The Environmental Protection Agency (EPA) recorded values of both iodine forms during the accident as shown in Fig. 5. The relative amounts of gaseous ^{131}I to total ^{131}I was reasonably constant at approximately 81%, roughly a factor of 4 difference between gaseous and particulate iodine. This value is similar to other studies based on the Chernobyl Nuclear Power Plant (NPP) accident and agrees closely with other studies based on Fukushima data such as the European value of 77.2% and a somewhat lower value in Japan of 68% (Masson et al., 2011). This factor was used to scale Canadian CTBT and national monitoring sites ^{131}I particulate measurements to total (gaseous plus particulate) ^{131}I values.

Looking at the system model in Fig. 4, the rate equations for the atmospheric deposition can be written as in Equation (1).

$$-\frac{d[Cs_p]}{dt} = k_{Cs_p}[Cs_p] - \frac{d[I_p]}{dt} = k_{I_p}[I_p] - k_{I_{gp}}[I_g] \quad (1)$$

Where the species in square brackets are the activity concentration in air for the particulate form, p, and gaseous form, g. The rate constants for the state of each species is given by k using the same subscripts, (e.g. $k_{I_{gp}}$ is the iodine rate constant for the conversion from gas to particulate). These e-folding equations, describe the duration for the atmospheric concentration to be reduced by a factor of e with the lifetime of the aerosol in the atmosphere determined by $1/k$.

$$-\frac{d[I_p]}{dt} = (k_{Cs_p} - 4k_{I_g})[I_p] \quad (2)$$

Equation (2) can then be solved for the aerosol atmospheric residence time, τ, for both isotopes, under the assumption that ^{131}I has a similar particle size distribution to ^{137}Cs, and is therefore scavenged at the same rate. Using this assumption, the residence times are given in Equation (3). Thus, these equations relate the removal processes of deposition and scavenging (both in-cloud and below) to the airborne aerosol concentrations. However, with the ongoing iodine conversion process, the particle size distribution assumption is not fully valid, as the newly formed particulate iodine begins to aggregate with other aerosols while the ^{137}Cs has no such phase conversion to model. Modelling such behaviour is currently beyond the capabilities of ATDM used in this study.

$$\tau_{Cs_p} = \frac{1}{k_{Cs_p}}\tau_{I_p} = \frac{1}{k_{I_p} - 4k_{I_g}} \approx \frac{1}{k_{Cs_p} - 4k_{I_g}} \quad (3)$$

With the model and equations now described, we now describe how the environmental model was applied. In this study, a modified type of box model was used over the entire domain of the North American continent. To improve the fitting of the measured data, all particulate concentrations were normalized by the activity concentration of ^{133}Xe (decay corrected to reference time) measured by the co-located xenon sampler. After the relative activity concentrations were calculated, they were rank ordered on a daily basis, regardless of geographical location. In effect, the plume was modelled as a continental-wide oscillating cloud where the relative ordering of the data was more important than the physical (measurement) location. The plume can also be viewed as a cloud which mixed very inefficiently throughout the time period (nine weeks) of this study. The mean of each rank were then weighted by the standard error, to derive an overall weighted residence time, and a 2σ (95%) confidence interval was calculated to provide a bounding estimate on the residence time.

3. Results and discussion

Using this first order kinetic model, the residence time of the measurement data from the sites in Fig. 2 were compared to the values produced by the MLDP ATDM. To ensure model fidelity, only the free decay period was used (no transient injects were allowed during the accident evolution), and the model results were used until before the normal ^{133}Xe background was re-established. Initially, ^{137}Cs was examined as it was much simpler to model as it did not have the gas-particulate phase conversion interaction during transit to consider.

Recalling from the section on collection and deposition, the activity concentrations were all referenced to the initial time of the accident. By plotting all observed IMS activity concentrations of ^{137}Cs and normalizing them by the ^{133}Xe activity concentration as shown in Fig. 6, any deviation from a zero slope in the exponential fit is due to debris being deposited on the ground through wet or dry deposition processes. To partially remove noise from the fitting process, only the first four ranks were considered when deriving a weighted removal rate coefficient. From the measured data, the mean atmospheric residence time, τ_{meas}, of ^{137}Cs was 11.71 d.

Now that the atmospheric removal rate coefficient has been determined from the field measurements, it was then used as a comparison with the MLDP dispersion model of the atmospheric residence time. Fig. 7 shows the results of using the empirically derived removal coefficient with the CMC global atmospheric inventory (black triangles) of ^{137}Cs. The model and measurements agree almost exactly up until roughly 57 d post-accident before there is a small underestimation in the deposited debris. Furthermore, the high degree of similarity between the two sets of data suggests that the oscillating cloud and rank order treatment of the measured data was a reasonable modelling approach, and the deposition simulation was reasonably accurate for an extended time post-accident, and could be reliably used in similar circumstances. The overall atmospheric residence time of 11.71 d for the measured ^{137}Cs data compares very closely with the ATDM derived residence time of 13.27 d. In the Chernobyl study, the residence time was found to be 3 d to 5 d (Uematsu et al., 1988), and a comprehensive study of aerosol

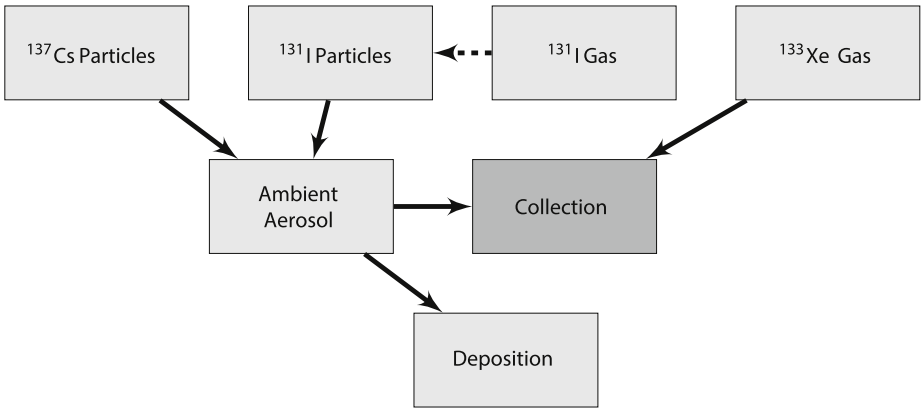

Fig. 4. A simple kinetic model of the behaviour of the ^{131}I, ^{133}Xe and ^{137}Cs radionuclides released into the air from the Fukushima reactor accident. Radioxenon is only removed through radioactive decay, caesium attaches to ambient aerosols and is removed through the process of wet and dry deposition, while iodine exists in both gaseous and particulate forms with a complex interplay between the two forms. At the collection site, the aerosol or radioxenon gas is collected and measured to determine the activity concentration in the sample.

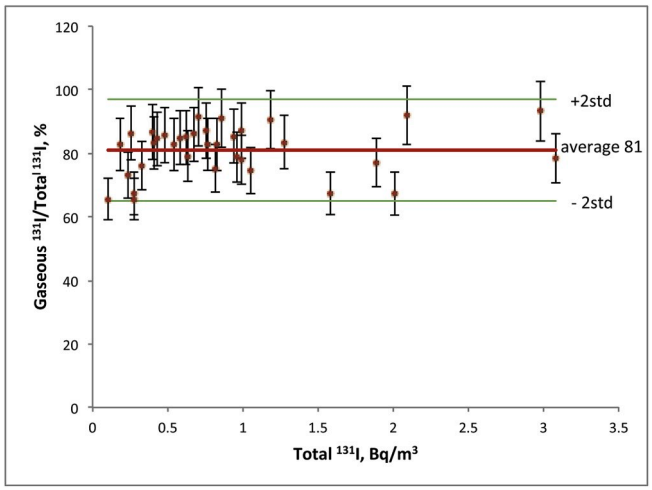

Fig. 5. Gaseous to Total ^{131}I ratio in the atmosphere observed in the US following the Fukushima NPP accident (retrieved from US EPA website http://www.epa.gov/enviro/facts/radnet/customized.html. The gaseous-to-total ratio of ^{131}I remained reasonably constant, at 81%, at US monitoring sites from islands in the Pacific to the Eastern seaboard of North America.

residence time based upon models and observations had overall ranges of 4 d to a month depending on the origin of the radioactive material (cosmogenic/stratosphere versus troposphere) (Giorgi and Chameides, 1986). However, a comprehensive study of Fukushima aerosols derived a residence time of between 10 d and 14 d (Kristiansen et al., 2016) which is consistent with this study. The difference between Fukushima and Chernobyl atmospheric residence time may be explained by enhanced wet deposition from below cloud scavenging with associated measurements occurring near the release point during the Chernobyl accident. In contrast, for this study, with much more distant measurement locations, most of the scavenging would have been in-cloud. Further studies would be necessary to confirm this behaviour.

With the residence time coefficient determined, ATDM could then be used to generate a North American continental ^{137}Cs deposition map as shown in Fig. 8. This deposition map was compared with the data that was collected by the United States Geological Survey (USGS) and was found to be in general agreement with the reported measurements (Wetherbee et al., 2012a, 2012b). This map was then used to assess the impact on health across Canada and formed a basis for the official Health Canada (HC) report.[1]

For ^{131}I, the atmosphere residence time calculation is more complicated due to the two phases of the radioiodine debris. While the particulate debris is being scavenged the gaseous iodine is nucleating and replenishing the particulate. By plotting the measured particulate iodine using rank ordering (same as ^{137}Cs) as shown in Fig. 9, the overall residence time can be directly calculated (assuming pure particulate ^{131}I is scavenged at the same rate as ^{137}Cs). Only the 3 highest ranked observations were used in this model due to the inconsistencies between the slope of the first 4th rank values and the data of higher rank. The overall residence time of 15d can now be used to assess the gaseous conversion lifetime. Applying Equation (3) from the kinetic model gives the mean phase transition as 27 d. The Chernobyl study reported a phase transition time of 14 d to 21 d (Uematsu et al., 1988).

Following the same procedure as was done for ^{137}Cs, a North American deposition map was generated for particulate deposition of ^{131}I. Due to the complexity of the iodine behaviour it was not possible to model the particulate replenishment process. In this case, the source term was scaled by a factor of 4 to account for the gaseous to particulate conversion as an imperfect solution as the atmospheric conversion time of the iodine could not be implemented. This leads to an overestimation of the total deposited iodine due to two factors: the simplification of the replenishment process, and the decay of deposited ^{131}I. Further work would be required to examine both effects more closely to understand their combined impact. The resulting map is shown in Fig. 10.

One last element of the study was to examine the mass-balance of the deposition simulation when considering the input source term mass and that of the deposited material. In order to examine mass balance, it is necessary to consider the global (or Northern Hemisphere) impact of the radioactive plume, and not just the North American continent. The input source term for ^{137}Cs, airborne concentration, surface deposition (including deposition onto both water and land) and the sum of the airborne and surface deposition were examined as shown in Fig. 11. From this analysis, it is clear that mass was conserved in the MLDP model. This analysis was performed only for ^{137}Cs due to the short half-life of ^{131}I. Furthermore, as the ATDM used was identical for both radionuclides, this conclusion would apply to both radionuclides.

4. Conclusion

This work successfully demonstrated a technique to estimate deposition at long range and over broad geographic scales using data provided by a sparse radionuclide detection network combined with ATDM.

[1] The complete HC report on the Fukushima Reactor accident and its impacts on Canada is available at: http://publications.gc.ca/site/eng/9.801801/publication.html.

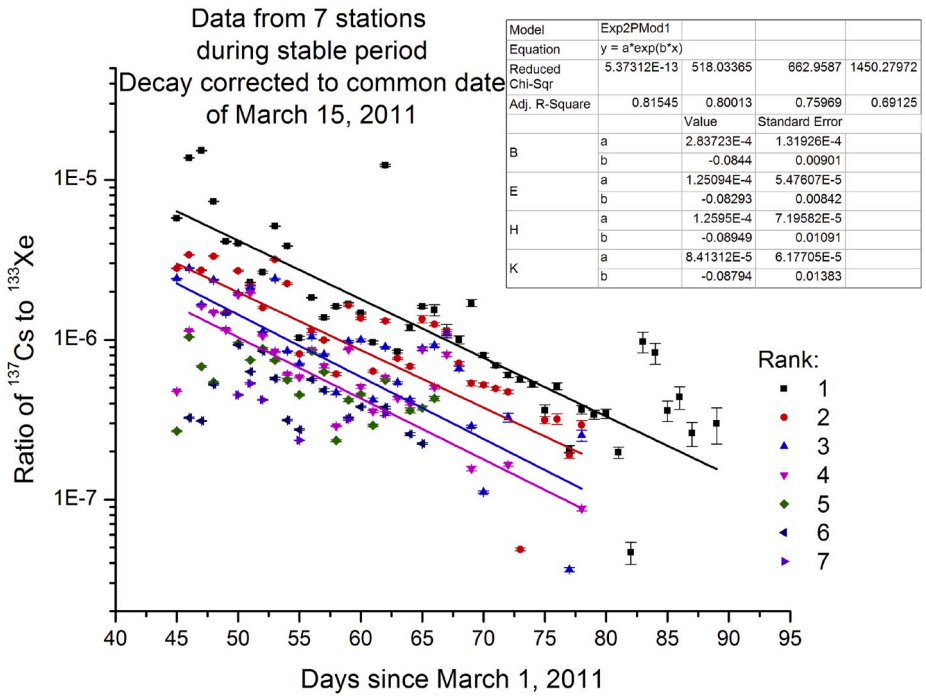

Fig. 6. Measurements of ^{137}Cs. Measurements from all monitoring sites with noble gas technology were collected and ordered by rank with the fitting parameters for the first four ranks (B, E, H, K) respectively. The weighted mean residence time was 11.71 d with a 95% confidence interval (10.50, 13.22).

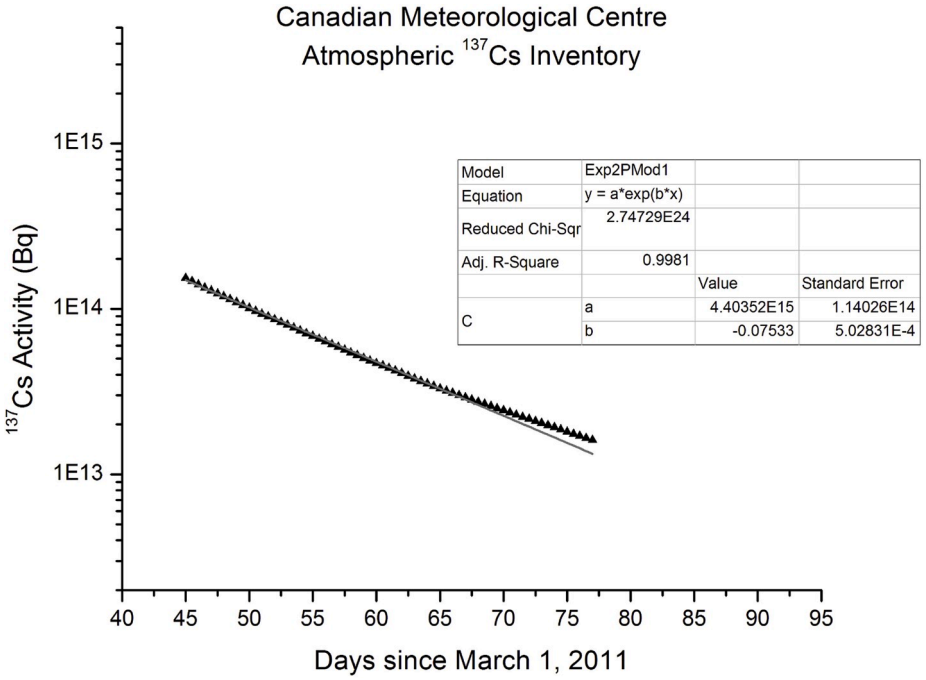

Fig. 7. Model of the Atmospheric Inventory of ^{137}Cs. The overall (empirical) weighted residence time for ^{137}Cs derived from Fig. 6 (light grey bottom series) compared to the MLDP deposition model (black triangles top series). The residence times were: $\tau_{meas} = 11.71\ d$ with a 95% confidence interval (10.50, 13.22) and from the MLDP ATDM $\tau_{model} = 13.27\ d$ with a 95% confidence interval (13.10, 13.45).

The use of co-located noble gas measurement values was useful as a non-depositing normalization technique to improve the accuracy of atmospheric residence time calculations.

The residence times for ^{137}Cs was determined using two different approaches, either through direct measurement in which case $\tau_{meas} = 12\ d$ or through a ATDM model run which resulted in $\tau_{model} = 13\ d$. The measured and modelled residence time were found to be comparable up until around 57 d post-accident.

The atmospheric residence time of ^{131}I was more difficult to determine as HC and IMS monitoring networks do not perform any gaseous iodine measurements. Data sets that allow for an estimate of the conversion process between particulate and gaseous phases are very limited and made the atmospheric residence time determination much more difficult. Furthermore, the MLDP model is not able to calculate decay of

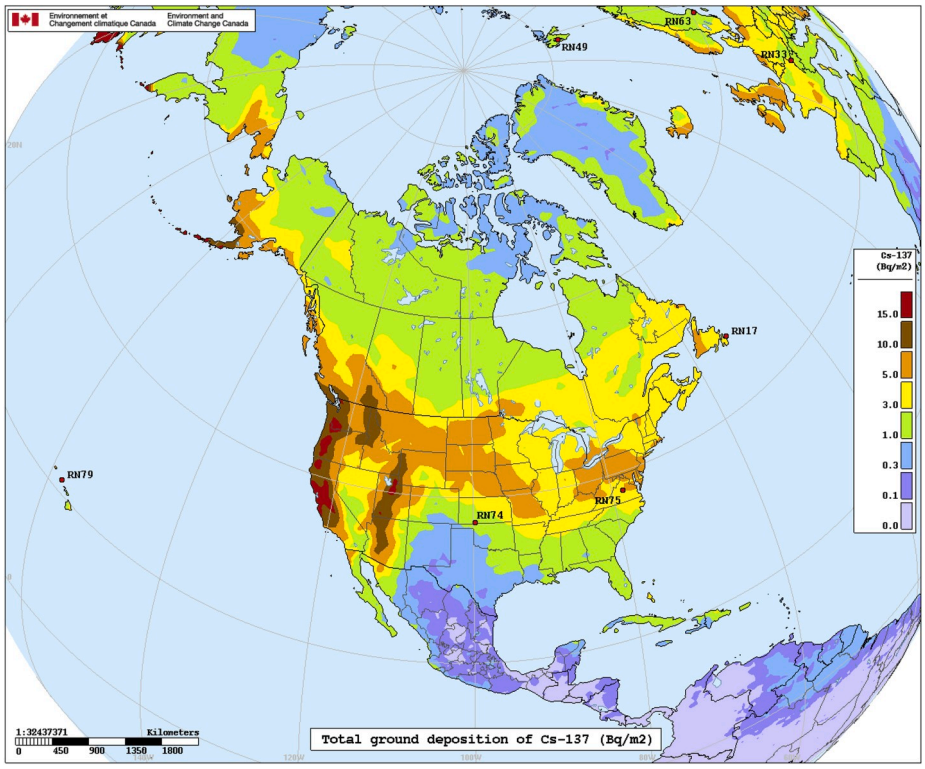

Fig. 8. Total ground deposition map over North America of ^{137}Cs (Bq m^{-2}) modelled with MLDP nine weeks after the start of release. Red dots represent CTBTO IMS measurement stations that were used in the study. (For interpretation of the references to colour in this figure legend, the reader is referred to the Web version of this article.)

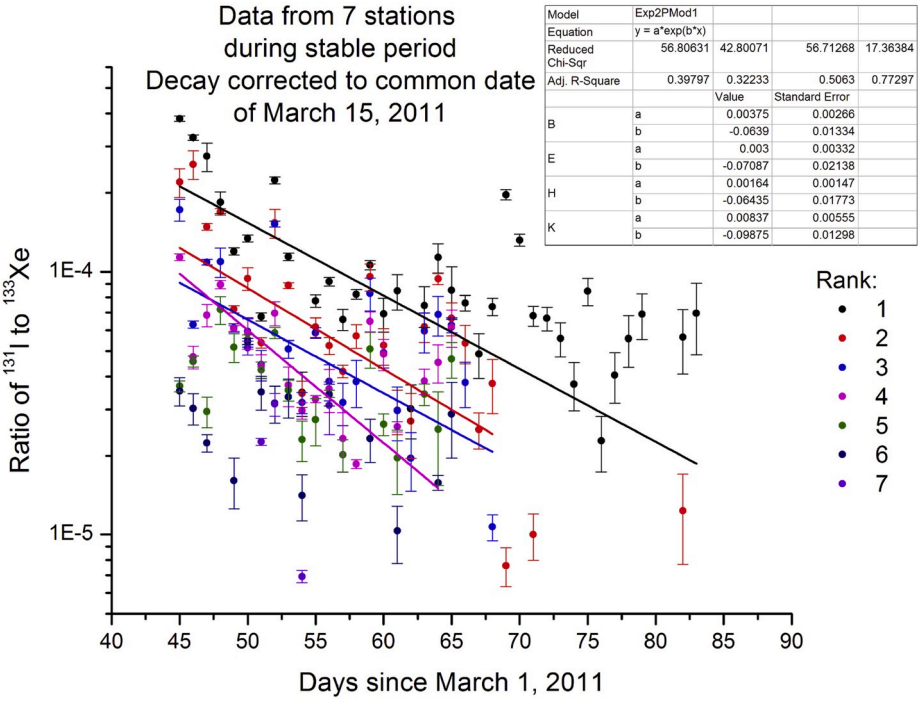

Fig. 9. Measurements of ^{131}I. The rank ordered ^{131}I measurement data was also weighted and fit with an exponential model to derive the overall atmospheric residence time for particulate ^{131}I. For ^{131}I, the weighted mean approximate τ_{meas} was 12.97 d with a 95% confidence interval (10.85, 16.12).

deposited radionuclides. Nevertheless, the overall atmospheric residence time was determined to be 15 d with a mean phase transition time of 27 d. This value is closer to the ratio derived residence time from the Chernobyl accident of 20 d. as compared to the direct estimate of 13 d (Uematsu et al., 1988). Some of the differences between the Chernobyl study and this Fukushima study may be due to the use of a generic dilution or mixing factor based upon an assessment of continental ^{222}Rn transport rather than a full atmospheric transport model.

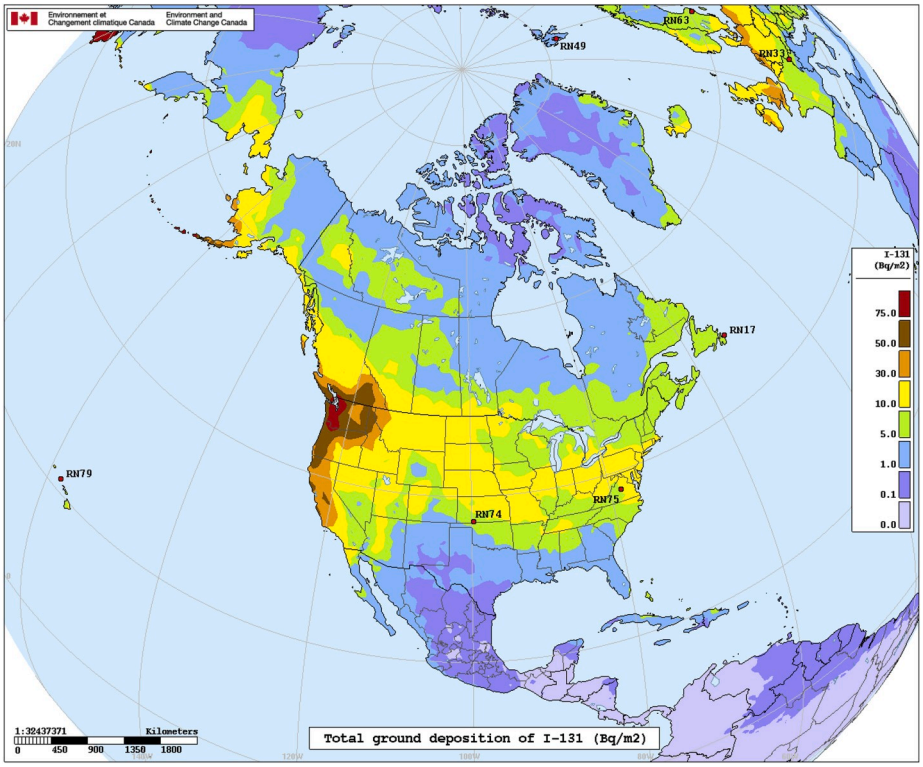

Fig. 10. Total ground deposition map over North America of ^{131}I (Bq m^{-2}) modelled with MLDP nine weeks after the start of release. Red dots represent CTBTO IMS measurement stations that were used in the study. This deposition map includes only the contribution of particulate ^{131}I. The gas to particle conversion is a complex process which was not able to be modelled. (For interpretation of the references to colour in this figure legend, the reader is referred to the Web version of this article.)

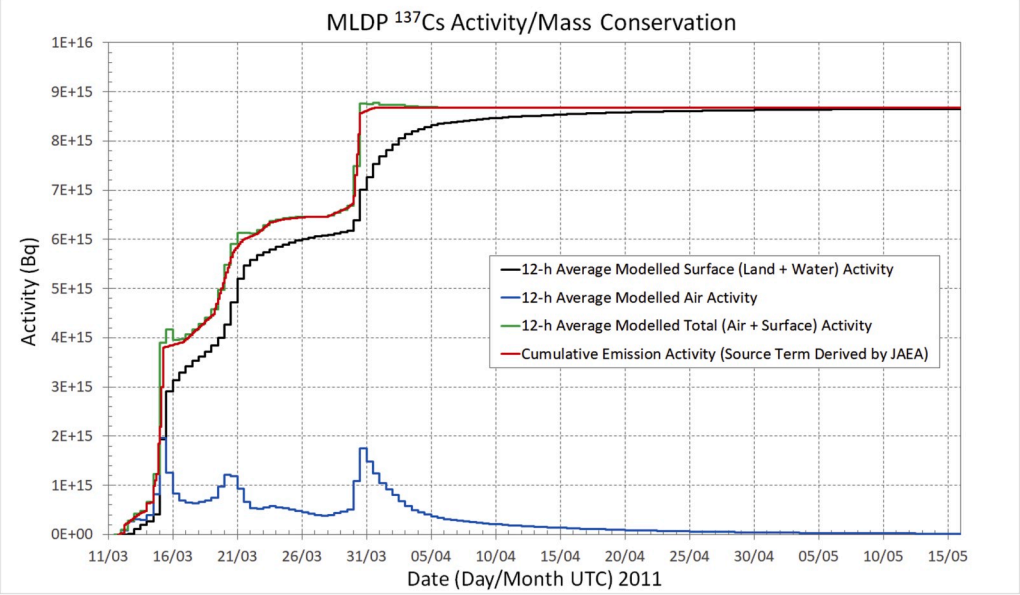

Fig. 11. Analysis of ATDM mass balance over the hemispheric computational model grid described in Fig. 3 for the 65.25 d simulation period.

The deposition maps generated for ^{137}Cs are well aligned with the deposition values recorded by the USGS. This suggests that the use of ATDM is reliable enough to be solely used to predict the deposition of ^{137}Cs in an operational setting. The deposition of ^{131}I did not show the same level of agreement with the USGS values, but was very similar to those determined for the Chernobyl accident. The lack of agreement with the USGS measurements is likely due to the complex behaviour of radioiodine in the atmosphere, and would perhaps require a more sophisticated kinetic model, including particle decay and the inclusion of atmospheric chemistry to provide better agreement before a purely modelled deposition would be satisfactory in an accident response environment.

Declaration of competing interest

The authors declare that they have no known competing financial interests or personal relationships that could have appeared to influence the work reported in this paper.

CRediT authorship contribution statement

I. Hoffman: Conceptualization, Methodology, Data curation, Investigation, Formal analysis, Writing - original draft, Visualization. **A. Malo:** Methodology, Visualization, Writing - review & editing. **P. Mekarski:** Visualization, Investigation, Formal analysis. **J. Yi:** Investigation, Formal analysis. **W. Zhang:** Investigation, Formal analysis. **N. Ek:** Methodology, Formal analysis. **P. Bourgouin:** Supervision. **G. Wotawa:** Methodology. **K. Ungar:** Methodology, Supervision.

Appendix A. Supplementary data

Supplementary data to this article can be found online at https://doi.org/10.1016/j.aeaoa.2020.100072.

References

Chino, M., Nakayama, H., Nagai, H., Terada, H., Katata, G., Yamazawa, H., 2011. Preliminary estimation of release amounts of ^{131}I and ^{137}Cs accidentally discharged from the Fukushima Daiichi nuclear power plant into the atmosphere. J. Nucl. Sci. Technol. 48 (7), 1129–1134. https://doi.org/10.1080/18811248.2011.9711799 arXiv:10.1080/18811248.2011.9711799.

Draxler, R., Arnold, D., Chino, M., Galmarini, S., Hort, M., Jones, A., Leadbetter, S., Malo, A., Maurer, C., Rolph, G., Saito, K., Servranckx, R., Shimbori, T., Solazzo, E., Wotawa, G., 2015. World Meteorological Organization's model simulations of the radionuclide dispersion and deposition from the Fukushima Daiichi nuclear power plant accident. J. Environ. Radioact. 139, 172–184. https://doi.org/10.1016/j.jenvrad.2013.09.014. http://www.sciencedirect.com/science/article/pii/S0265931X13002142.

D'Amours, R., Malo, A., Flesch, T., Wilson, J., Gauthier, J.-P., Servranckx, R., 2015. The Canadian meteorological centre's atmospheric transport and dispersion modelling suite. Atmos.-Ocean 53 (2), 176–199. https://doi.org/10.1080/07055900.2014.1000260.

Evangeliou, N., Balkanski, Y., Florou, H., Eleftheriadis, K., Cozic, A., Kritidis, P., 2015. Global deposition and transport efficiencies of radioactive species with respect to modelling credibility after Fukushima (Japan, 2011). J. Environ. Radioact. 149, 164–175. https://doi.org/10.1016/j.jenvrad.2015.07.024. http://www.sciencedirect.com/science/article/pii/S0265931X15300667.

Giorgi, F., Chameides, W.L., 1986. Rainout lifetimes of highly soluble aerosols and gases as inferred from simulations with a general circulation model. arXiv J. Geophys. Res.: Atmospheres 91 (D13), 14367–14376. https://doi.org/10.1029/JD091iD13p14367. https://agupubs.onlinelibrary.wiley.com/doi/pdf/10.1029/JD091iD13p14367. https://agupubs.onlinelibrary.wiley.com/doi/abs/10.1029/JD091iD13p14367.

Katata, G., Chino, M., Kobayashi, T., Terada, H., Ota, M., Nagai, H., Kajino, M., Draxler, R., Hort, M., Malo, A., Torii, T., Sanada, Y., 2015. Detailed source term estimation of the atmospheric release for the Fukushima Daiichi Nuclear Power Station accident by coupling simulations of atmospheric dispersion model with improved deposition scheme and oceanic dispersion model. Atmos. Chem. Phys. 15, 1029–1070. https://doi.org/10.5194/acp-15-1029-2015.

Korsakissok, I., Mathieu, A., Didier, D., 2013. Atmospheric dispersion and ground deposition induced by the Fukushima Nuclear Power Plant accident: a local-scale simulation and sensitivity study. Atmos. Environ. 70, 267–279. https://doi.org/10.1016/j.atmosenv.2013.01.002. http://www.sciencedirect.com/science/article/pii/S1352231013000083.

Kristiansen, N.I., Stohl, A., Olivié, D.J.L., Croft, B., Søvde, O.A., Klein, H., Christoudias, T., Kunkel, D., Leadbetter, S.J., Lee, Y.H., Zhang, K., Tsigaridis, K., Bergman, T., Evangeliou, N., Wang, H., Ma, P.-L., Easter, R.C., Rasch, P.J., Liu, X., Pitari, G., Di Genova, G., Zhao, S.Y., Balkanski, Y., Bauer, S.E., Faluvegi, G.S., Kokkola, H., Martin, R.V., Pierce, J.R., Schulz, M., Shindell, D., Tost, H., Zhang, H., 2016. Evaluation of observed and modelled aerosol lifetimes using radioactive tracers of opportunity and an ensemble of 19 global models. Atmos. Chem. Phys. 16 (5), 3525–3561. https://doi.org/10.5194/acp-16-3525-2016. https://www.atmos-chem-phys.net/16/3525/2016/.

Lebel, L.S., Dickson, R.S., Glowa, G.A., Lebel, L.S., Dickson, R.S., Glowa, G.A., 2016. Radioiodine in the atmosphere after the Fukushima Dai-ichi nuclear accident. J. Environ. Radioact. 151, 82–93. https://doi.org/10.1016/j.jenvrad.2015.06.001. http://www.sciencedirect.com/science/article/pii/S0265931X1530014X.

Masson, O., Baeza, A., Bieringer, J., Brudecki, K., Bucci, S., Cappai, M., Carvalho, F., Connan, O., Cosma, C., Dalheimer, A., Didier, D., Depuydt, G., Geer, L.D., Vismes, A. D., Gini, L., Groppi, F., Gudnason, K., Gurriaran, R., Hainz, D., Halldórsson, Ó., Hammond, D., Hanley, O., Holeý, K., Homoki, Z., Ioannidou, A., Isajenko, K., Jankovic, M., Katzlberger, C., Kettunen, M., Kierepko, R., Kontro, R., Kwakman, P., Lecomte, M., Vintro, L.L., Leppänen, A.-P., Lind, B., Lujaniene, G., Ginnity, P.M., Mahon, C.M., Malá, H., Manenti, S., Manolopoulou, M., Mattila, A., Mauring, A., Mietelski, J., Møller, B., Nielsen, S., Nikolic, J., Overwater, R., Pálsson, S.E., Papastefanou, C., Penev, I., Pham, M., Povinec, P., Ramebäck, H., Reis, M., Ringer, W., Rodriguez, A., Rulík, P., Saey, P., Samsonov, V., Schlosser, C., Sgorbati, G., Silobritiene, B.V., Söderström, C., Sogni, R., Solier, L., Sonck, M., Steinhauser, G., Steinkopff, T., Steinmann, P., Stoulos, S., Sýkora, I., Todorovic, D., Tooloutalaie, N., Tositti, L., Tschiersch, J., Ugron, A., Vagena, E., Vargas, A., Wershofen, H., Zhukova, O., 2011. Tracking of airborne radionuclides from the damaged Fukushima Dai-Ichi nuclear reactors by European networks. Environ. Sci. Technol. 45 (18), 7670–7677. https://doi.org/10.1021/es2017158 pMID: 21809844. arXiv, URL.

Morino, Y., Ohara, T., Nishizawa, M., 2011. Atmospheric behavior, deposition, and budget of radioactive materials from the Fukushima Daiichi nuclear power plant in March 2011. Geophys. Res. Lett. 38 (7), l00G11. https://doi.org/10.1029/2011GL048689.

Terada, H., Katata, G., Chino, M., Nagai, H., 2012. Atmospheric discharge and dispersion of radionuclides during the Fukushima Dai-ichi Nuclear Power Plant accident. Part II: verification of the source term and analysis of regional-scale atmospheric dispersion. J. Environ. Radioact. 112, 141–154. https://doi.org/10.1016/j.jenvrad.2012.05.023.

Uematsu, M., Merrill, J.T., Patterson, T.L., Duce, R.A., Prospero, J.M., 1988. Aerosol residence times and iodine gas/particle conversion over the North Pacific as determined from Chernobyl radioactivity. Geochem. J. 22 (4), 157–163. https://doi.org/10.2343/geochemj.22.157.

Wetherbee, G.A., Gay, D.A., Debey, T.M., Lehmann, C.M.B., Nilles, M.A., 2012a. Wet deposition of fission-product isotopes to North America from the Fukushima Dai-ichi incident, March 2011. Environ. Sci. Technol. 46 (5), 2574–2582. https://doi.org/10.1021/es203217u doi: 10.1021/es203217u.

Wetherbee, G., Debey, T., Nilles, M., Lehmann, C., Gay, D., 2012b. Fission Products in National Atmospheric Deposition Program—Wet Deposition Samples Prior to and Following the Fukushima Dai-Ichi Nuclear Power Plant Incident, March 8–April 5, 2011, Tech. Rep. 2011–1277. U.S. Geological Survey.